

Ultrafast optical studies of ordered poly(3-thienylene-vinylene) films

E. Olejnik,¹ B. Pandit,¹ T. Basel,¹ E. Lafalce,² C.-X. Sheng,^{1,*} C. Zhang,³ X. Jiang,^{2,†} and Z. V. Vardeny¹

¹*Department of Physics & Astronomy, University of Utah, Salt Lake City, Utah 84112, USA*

²*Department of Physics, University of South Florida, Tampa, Florida 33620, USA*

³*Department of Chemistry & Biochemistry, South Dakota State University, Brookings, South Dakota 57007, USA*

(Received 25 January 2012; revised manuscript received 9 May 2012; published 12 June 2012)

Using femtosecond transient photomodulation, photoluminescence, and electro-absorption spectroscopies, we studied the ultrafast photoexcitation dynamics and nonlinear optical properties of ordered poly(thienylene-vinylene) (PTV), which belongs to a rare class of nonluminescent, nondegenerate-ground-state π -conjugated polymers. We show that the ordered PTV films contain abundant nanocrystalline domains that substantially influence the optical spectra as a result of aggregates formation. We demonstrate that the primary intrachain exciton (1^1B_u) decays within ~ 500 fs to the more stable “dark” exciton (2^1A_g), and the released energy results in both static strain and propagating strain wave that bounces back and forth in the polymer film.

DOI: [10.1103/PhysRevB.85.235201](https://doi.org/10.1103/PhysRevB.85.235201)

PACS number(s): 78.47.J-, 78.66.Qn, 78.40.Me, 78.45.+h

The π -conjugated polymers may be divided into two principal classes: namely, polymers with degenerate ground state, and polymers with nondegenerate ground state (NDGS).¹ Usually NDGS polymers have high photoluminescence (PL) quantum efficiency (PLQE), and thus may be attractive for organic light-emitting diodes.² The ultrafast photoexcitation dynamics of luminescent NDGS polymers are well understood. Upon photon absorption into a high-energy singlet exciton, there is an ultrafast thermalization to the lowest exciton, namely, the 1^1B_u exciton, followed by PL or recombination via nonradiative channels.³ In rare occasions, NDGS polymers have weak PL emission; poly(thienylene-vinylene) (PTV) (see Fig. 1) is such a polymer.⁴ It has a lower optical gap (1.7–1.8 eV) compared to other NDGS polymers and thus could, in principle, provide a better match with the solar spectrum for organic solar cell applications.^{5,6} However, so far PTV-based solar cells have shown low power-conversion efficiency, indicating poor charge photogeneration.⁷

Low PLQE may be *extrinsic* in origin, where the photogenerated 1^1B_u exciton falls into traps. Alternatively, it has been proposed that low *intrinsic* PLQE in π -conjugated polymers results from the order of the electronic excited states.^{1,8} In this model, if the lowest even-parity (dark) exciton, or 2^1A_g , lies below the 1^1B_u exciton (i.e., $E[2^1A_g] < E[1^1B_u]$), it may circumvent the PL emission. In this case, according to Kasha’s rule, the photogenerated 1^1B_u exciton undergoes ultrafast internal conversion to the dark 2^1A_g exciton, thus eliminating further PL emission. This process, however, has not been yet identified in PTV, and thus the origin of its weak PL emission is still unclear; it might be extrinsic or intrinsic in origin.

Moreover, in NDGS polymers with weak intrinsic PL, there is a substantial amount of energy that is released very fast via the $1^1B_u \rightarrow 2^1A_g$ internal conversion process and subsequent 2^1A_g decay to the ground state; this leads to thermal stress that is accompanied by transient strain.^{9,10} Thus, the fascinating phenomena that nonluminescent NDGS polymers may undergo upon photon absorption make them unique materials for ultrafast and nonlinear optical investigations. However, the photophysics of only few NDGS polymers have been studied in detail, where cis-(CH)_x¹¹ and polydiacetylene¹² are the exceptions.

In this work, we studied the ultrafast photophysics of a new form of PTV having superior order (see Fig. 1)¹³ that may increase the PLQE. For our studies, we used X-ray diffraction (XRD) and femtoseconds (fs) transient photomodulation (PM) in a broad spectral range, as well as continuous wave (cw) PL, and electro-absorption (EA) spectroscopies. The fs transient PM focuses on the primordial photoexcitations;³ the cw PL reveals the singlet exciton properties;¹⁴ and EA unravels the polymer essential excited states.^{8,15} We found that the ordered PTV films contain abundant nanocrystalline domains that influence the polymer cw and transient optical spectra as a result of aggregates formation.¹⁴ However, in spite of the improved order, the new PTV polymer still shows very small PLQE ($< 2 \times 10^{-4}$), and thus this polymer is *intrinsically* “dark.” We confirmed the order $E(2^1A_g) < E(1^1B_u)$ by studying the ultrafast PM dynamics, and we show that within a few hundred femtoseconds, the photogenerated 1^1B_u exciton decays into the “dark” 2^1A_g exciton, accompanied by photo-induced static strain and a dynamic strain wave in the film with periodic response dynamics.

The synthesis of the ordered PTV polymer with controlled regio-regularity (RR-) is described elsewhere.¹³ In this paper, we report our studies of RR-PTV with 100% regio-regularity, i.e., superior order [see Fig. 1(a)]. The RR-PTV powder was originally dissolved in dichlorobenzene (~ 10 mg/ml), and diluted to 0.01 mg/ml for “PTV in dilute solution.” Alternatively, the original solution was drop cast into films on sapphire and CaF₂ substrates to allow broadband optical spectroscopies. For comparison, we also used films of regio-random PTV (RRa-PTV), where the polymer side groups are randomly oriented.¹³

For the transient PM spectroscopy in the mid-infrared spectral range, we employed the fs two-color polarized pump-probe correlation technique using a low-power (energy/pulse ~ 0.1 nJ), high-repetition-rate (~ 80 MHz) laser system based on Ti:sapphire (Tsunami, Spectra-Physics), and an optical parametric oscillator (OPO; Opal, Spectra-Physics) that spans $\hbar\omega(\text{probe})$ from 0.24 to 1.1 eV.³ The pump beam (~ 100 fs pulse duration) was frequency doubled to $\hbar\omega(\text{pump}) = 3.1$ eV, and subsequently both pump and probe beams were focused on the sample film to a spot of ~ 50 μm , with resulting

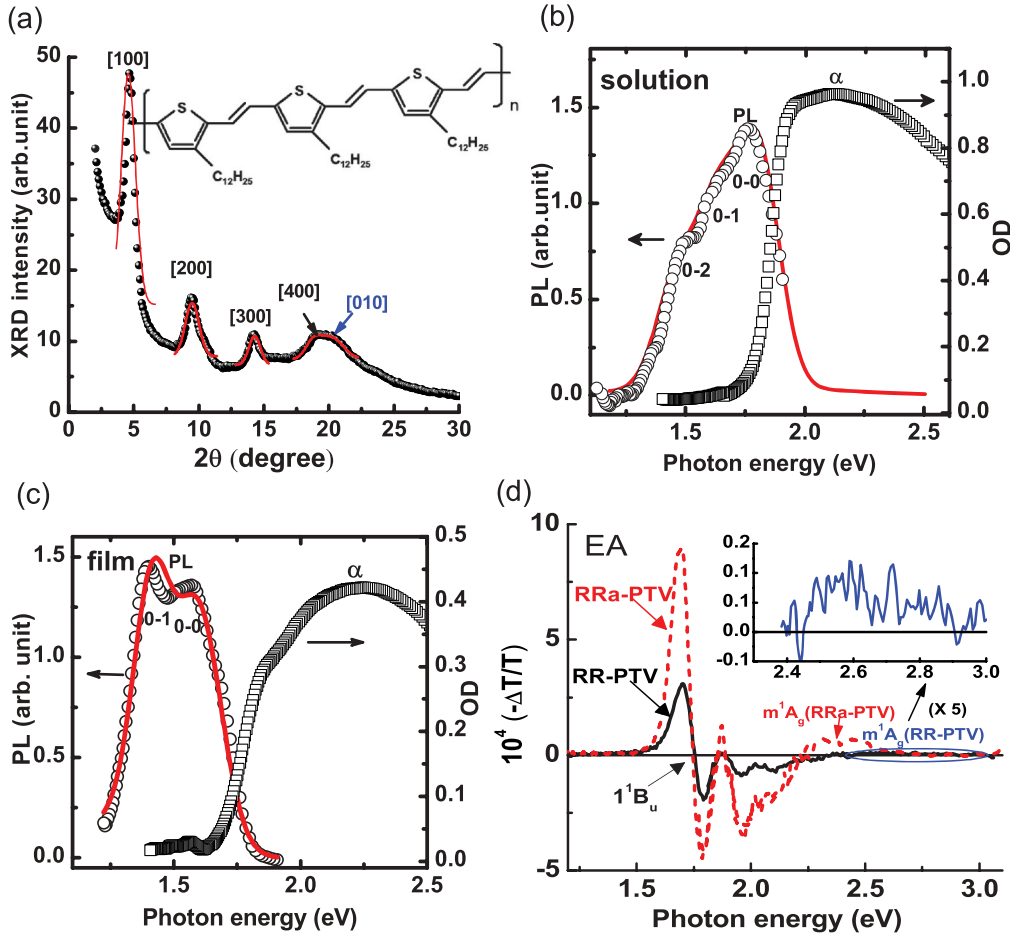


FIG. 1. (Color online) (a) The XRD pattern of a RR-PTV film showing the prominent out-of-plane [100] band and its harmonics, as well as an in-plane [010] band that shows lamellae formation;¹⁹ the red line drawn on the various bands is a Gaussian fit; the fourth peak is a sum of two Gaussians with different widths. The inset shows the backbone structure of the RR-PTV polymer. (b) The PL and absorption spectra of RR-PTV in dilute solution. The line through the data points is a fit using a modified Franck-Condon model (see text). (c) Same as in (b) but for RR-PTV film. Various vibronic transitions were labeled for clarity. (d) The EA spectra of RRa-PTV (dashed red line) and RR-PTV (full black line). The spectral EA features related to 1^1B_u and m^1A_g are assigned. The inset is a blow-up of the EA spectrum from 2.4 to 3.0 eV that includes the m^1A_g state.

photoexcitation density of $\sim 10^{16}/\text{cm}^3$. For the transient PM in the visible/near-infrared spectral range, we used a high-power (energy/pulse $\sim 10 \mu\text{J}$), low-repetition-rate ($\sim 1 \text{ kHz}$) fs laser system with pump $\hbar\omega(\text{pump}) = 3.1 \text{ eV}$ and $1.3 \text{ eV} < \hbar\omega(\text{probe}) < 2.5 \text{ eV}$ based on supercontinuum white light generation;³ in this case, the photoexcitation density was $\sim 5 \times 10^{17}/\text{cm}^3$. The transient PM was obtained from $\Delta T/T(t)$, in which ΔT is the change of transmission upon pump illumination, and $T(t)$ is the original transmission, using a phase-sensitive lock-in technique, where negative PM is due to photo-induced absorption (PA), and positive PM is due to photo-bleaching (PB). For retrieving the ultrafast response below the system temporal resolution of $\sim 150 \text{ fs}$, we analyzed the obtained PM transients using a convolution scheme of the transient response with the pump/probe cross-correlation function.¹⁶

The cw PL spectrum was measured using a standard setup,¹⁷ whereas the PLQE was measured with an integrated sphere.¹⁸ For the EA spectrum, we measured $\Delta T/T$ induced by the external electric field, using a lock-in amplifier set at $2f$ due to the field modulation at f . The PTV film was deposited

on a specially designed substrate that contained interdigitated electrodes.¹⁵

Figure 1(a) shows the “grazing incidence” XRD pattern of a RR-PTV film using the $\text{Cu}K\alpha$ X-ray line at $\lambda = 0.154 \text{ nm}$. The sharp band at $2\theta = 4.7^\circ$ [100] and its three harmonics show that there are abundant nanocrystalline domains in the ordered PTV films. In addition, the peak at 20.13° [010] is indicative of out of plane lamellar structures.¹⁹ Using the Scherrer relation and the XRD [100] bandwidth, we obtain an average domain size of 7 nm. This leads to the formation of H-aggregates in the crystalline domains, similar to regio-regular poly-[3-hexylthiophene] (RR-P3HT)^{14,19} films. In H-aggregates, the 0-0 transition in the PL emission ($1^1B_u \rightarrow 1^1A_g$) and absorption ($1^1A_g \rightarrow 1^1B_u$) is strictly forbidden, but in reality, it is only suppressed compared to the 0-1 phonon replica in the spectrum. In the following, we adopt the model advanced for aggregate emission in RR-P3HT,¹⁴ and parameterize the 0-0 “suppression degree” by a constant parameter, α ($0 < \alpha < 1$), where $\alpha < 1$ stands for H-aggregate PL spectrum, and $\alpha = 1$ represents the single-chain emission spectrum.

Figure 1(b) shows the absorption and PL spectra of RR-PTV in *dilute solution*, where the polymer chains are isolated. We measured a very low PLQE value, $\eta \sim 2 \times 10^{-4}$. The weak PL emission in solution form shows that it is an *intrinsic* property of the RR-PTV polymer influenced by the order $E(2^1A_g) < E(1^1B_u)$. We could fit the weak PL spectrum in solution using a modified Franck-Condon model that includes vibronic replica:¹⁴

$$I(\omega) \sim (\hbar\omega)^3 [\alpha\Gamma(\hbar\omega - E_0) + \sum (S^m/m!) \Gamma(\hbar\omega - (E_0 - mE_p))]. \quad (1)$$

In Eq. (1), S is the Huang-Rhys parameter, m is the number of the vibrational modes involved in the transition, E_0 is the PL onset at $\sim E(1^1B_u)$, E_p is the strongest coupled vibrational energy, and $\Gamma(\hbar\omega - E_0)$ is a Gaussian distribution function around E_0 having width of ~ 0.1 eV due to the disorder in the film. We fit the dilute PL spectrum using Eq. (1) with $E_0 = E(1^1B_u) = 1.8$ eV, $\alpha = 1$, $E_p = 0.18$ eV ($C = C$ stretching vibration), $S = 1.37$, and $m = 0, 1-3$ (see supplementary

material for the fitting of PL spectra).²⁰ The absorption spectrum could be also fit (not shown) using Eq. (1) with the same parameters as for the PL spectrum, but with a distribution of $E(1^1B_u)$ that corresponds to various polymer conjugation lengths in the film.¹⁵ We thus conclude that the optical spectra of RR-PTV in dilute solution originate from *isolated polymer chains*; in contrast, the optical spectra in RR-PTV films are influenced by *aggregates* in the nanocrystalline domains.

Figure 1(c) shows the PL and absorption spectra of ordered RR-PTV *film*. The PLQE is somewhat smaller than in solution, but its line shape is dramatically different than that in solution. It appears that the 0-0 transition has significantly red-shifted to 1.58 eV, and was suppressed in the film PL spectrum, and the absorption spectrum increases more gradually; both effects point to H-aggregates in the film.¹⁴ We explain the red shift of the 0-0 transition by the solid state effect, where the excitons in solid state simply red-shifted because of the change of dielectric constant. In fact, we could not fit the PL spectrum in RR-PTV film [Fig. 1(c)] using Eq. (1) with the same parameters as for PL in solution (see supplementary material

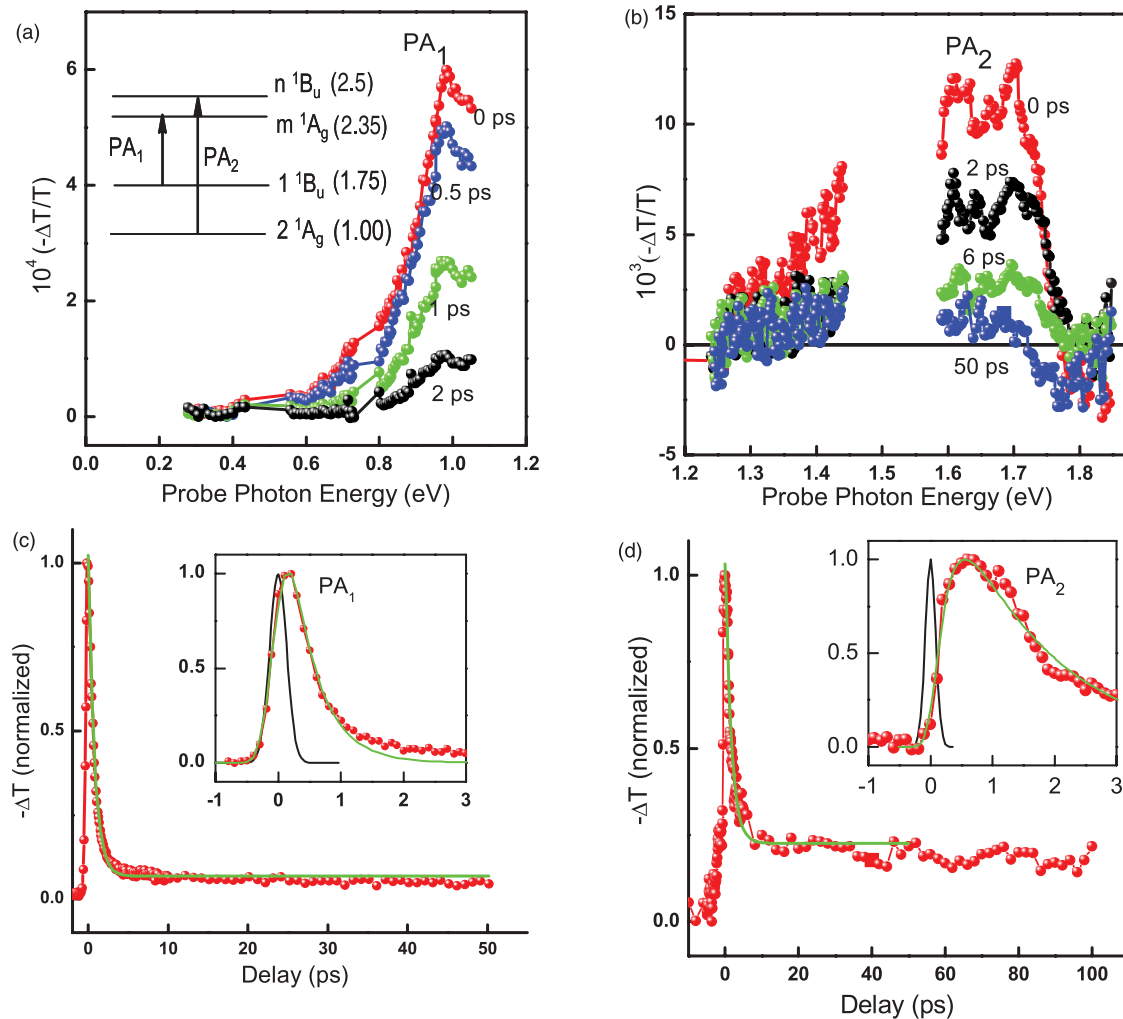


FIG. 2. (Color online) The transient PM spectrum of RR-PTV film measured at various delay times, t , in (a) mid-infrared spectral range and (b) visible/near-infrared spectral range; PA₁ and PA₂ bands are assigned. The inset to (a) is a schematic of the PTV essential states and associated optical transitions. (c) and (d) The respective decay dynamics of PA₁ at 0.95 eV and PA₂ at 1.6 eV. The insets to (c) and (d) focus on the PA formation and decay evolution near $t = 0$, where the data (red solid circles) are fitted with an exponential formation and decay processes (green line), taking into account the pump/probe cross-correlation function (black line).¹⁶

for the fitting of PL spectra).²⁰ The best fit yields $S = 0.90$, $E_0 = 1.58$ eV, and $\alpha = 0.80$, showing that the 0-0 transition is indeed suppressed due to the aggregates. We note that the PLQE in RRA-PTV is even smaller than that in RR-PTV.⁶

The EA spectra of RR- and RRA-PTV films are given in Fig. 1(d). Similar to EA spectra in many other polymers, the EA spectra show a derivative-like band around $E(1^1B_u)$ that is due to the Stark shift of the 1^1B_u exciton, followed by several vibration replicas and an absorption band at m^1A_g due to electric field-induced symmetry breaking.¹⁵ However, the m^1A_g band in RR-PTV is much smaller and broader than in RRA-PTV, indicating that the aggregates in this film also affect the EA spectrum. We postulate that the 0-0 transition in the $1^1B_u \rightarrow m^1A_g$ band, which determines the EA band at m^1A_g ,^{8,15} is partially suppressed in aggregates, so that the vibronic replicas in the m^1A_g EA band are relatively more apparent. In any case, from the dominant features in the EA spectrum, we obtain the energy levels of two important essential states,⁸ namely, $E(1^1B_u) \approx 1.75$ eV and $E(m^1A_g) \approx 2.55$ eV [at the onset of the EA m^1A_g band, see inset of Fig. 1(d)]. This determines the energy difference between these two states, $\Delta E = 0.8$ eV, a value that is essential for understanding the PA band that originates from the photogenerated 1^1B_u excitons in the film.³

Figures 2(a) and 2(b) show the transient PM spectra in RR-PTV film at various times t following pulse excitation. The PM spectrum is dominated by two PA bands, namely, PA_1 at ~ 0.95 eV and PA_2 at ~ 1.6 eV (both bands with broad tails toward lower energies), and a derivative-like feature having zero-crossing (isosbestic point) at ~ 1.75 eV. Figures 2(c) and 2(d) show the PA transient decays; it is clear that the two PA bands do not share the same dynamics. Whereas PA_1 decays almost completely within $\sim \frac{1}{2}$ ps, the decay of PA_2 is longer (~ 2.5 ps) into a plateau that indicates the formation of a relatively stable photoexcitation. We thus conclude that the two PA bands *do not belong to the same photoexcitation*. A closer inspection of the PA responses near $t = 0$ [insets to Figs. 2(c) and 2(d)] reveals that PA_1 is instantaneously generated, whereas PA_2 is formed at a delay of ~ 200 fs (see supplementary material for the cross-correlation analysis in transient PA spectra).²⁰ We therefore conclude that PA_2 does not originate from the primary photoexcitation in RR-PTV but rather is formed at the expense of PA_1 , and during its decay process.

The band PA_1 is generic to many π -conjugated polymers, and it has been previously identified³ as being due to optical transitions from the photogenerated 1^1B_u exciton into the m^1A_g exciton.⁸ Therefore, we infer that PA_1 in RR-PTV is also due to the photogenerated 1^1B_u exciton. Its ultrafast decay kinetics, however, indicate that there is another state at lower energy ($< E[1^1B_u]$), into which the photogenerated 1^1B_u exciton decays; this should be the elusive dark exciton, 2^1A_g . As a check of this proposed scenario, we estimate the PLQE from the fast 1^1B_u decay and compare it to the PLQE η -value measured by an integrated sphere. For this estimate, we used the relation: $\eta = \tau/\tau_{\text{rad}}$, where τ is the exciton lifetime, and τ_{rad} (~ 1 ns)²¹ is the 1^1B_u radiative lifetime. Using a PA_1 lifetime of $\sim \frac{1}{2}$ ps, we thus estimate $\eta(\text{PTV}) \approx 5 \times 10^{-4}$, which is in good agreement with the measured η -value ($\sim 2 \times 10^{-4}$). Within this decay scenario, PA_2 is a transition from the 2^1A_g state. This optical transition, however, should be

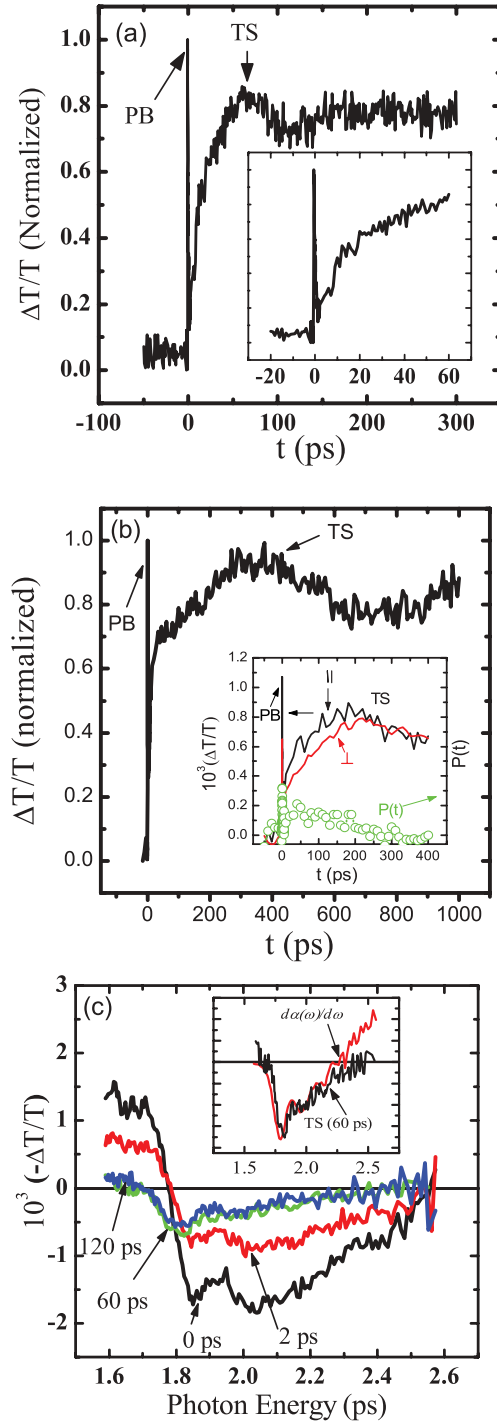


FIG. 3. (Color online) (a) and (b) The transient PM response at $\hbar\omega(\text{probe}) = 1.80$ eV of two RR-PTV films with different thicknesses: (a) $d \approx 60$ nm, and (b) $d \approx 330$ nm. The ultrafast electronic response (PB) and the transient strain (TS) response that show an oscillatory component are assigned. Note that the oscillation period, τ_T , is different in (a) and (b). The inset to (a) shows in more detail the PB decay and TS onset response for $d \approx 60$ nm; the inset in (b) shows $\Delta T(t)$ parallel (\parallel) and perpendicular (\perp) response dynamics and the resulting polarization degree, $P(t)$, for a film of $d \approx 210$ nm. (c) The PM spectra of RR-PTV film of $d \approx 60$ nm in the $\hbar\omega(\text{probe})$ interval 1.6–2.6 eV, which show the evolution of the PB response. The inset compares the PB spectrum at 60 ps (dominated by the TS response) with the spectrum of the absorption derivative, $d\alpha(\omega)/d\omega$.

into an odd-parity exciton, namely, the n^1B_u exciton, which is also part of the polymer essential states.⁸ The stabilization of PA_2 at later time ($t > 5$ ps) into a plateau indicates that some of the 2^1A_g excitons become trapped, similar to the classic polymer t-(CH)_x.²² As the consequence of the two transient PA bands, and the cw PL and the EA spectrum, we construct the essential-states structure and related optical transitions in PTV in the Fig. 2(a) inset.

Figure 3(c) shows the initial PB spectrum and its time evolution. The PB spectrum at $t = 0$ has similar features as in the absorption spectrum of the film [Fig. 1(c)]; there is a prominent PB band at 1.85 eV (1^1B_u), followed by a phonon side band at ~ 2.03 eV. However, at $t > 10$ ps, the PB spectrum dramatically changes; it does not resemble the absorption spectrum any longer, but rather follows the absorption derivative spectrum, $d\alpha(\omega)/d\omega$ [see Fig. 3(c), inset]. At the same time, $\Delta T(t)$ near the isosbestic point at $\hbar\omega = 1.80$ eV starts increasing [Fig. 3(a), inset], showing the onset of a second ΔT component. In addition, we found that $\Delta T(t)$ is initially polarized, having polarization degree $P \sim \frac{1}{2}$, where $P = (\Delta T_{\parallel} - \Delta T_{\perp})/(\Delta T_{\parallel} + \Delta T_{\perp})$. However, at $t > 10$ ps, $P(t)$ decays quickly to $P = 0$, which is reached at the peak of the second $\Delta T(t)$ component [Fig. 3(b), inset]. In addition to a marked plateau that is reached at ~ 60 ps [Fig. 3(a), inset], there is also a superposed oscillatory component [Figs. 3(a) and 3(b)]. We note that the oscillation period, τ_T , depends on the film thickness, d ; we measure $\tau_T \approx 120$ ps for a film thickness $d \approx 60$ nm [Fig. 3(a)], and $\tau_T \approx 650$ ps for a thicker film of $d \approx 330$ nm [Fig. 3(b)]. We therefore conclude that the second $\Delta T(t)$ component contains a *propagating wave* response that bounces back and forth in the film, due to successive reflection at the two film boundaries with τ_T determined by the “round-trip” time.

The second $\Delta T(t)$ component is not electronic in origin. This transient response is not polarized, bounces back and forth inside the film, and is formed at the expense of the electronic PB response. These facts, taken together, unravel its origin as due to thermal stress that launches a propagating strain wave in the film, i.e., transient strain (TS).^{9–11} The spatial and temporal dependencies of the TS, $\eta(z, t)$, can be derived by solving a one-dimensional wave equation, with a thermal generation term for a semitransparent film.⁹ Assuming zero displacement at the film boundary at $z = 0$,

$$\begin{aligned}\eta(z, t) &= K[e^{-z/\xi}(2 - e^{-vt/\xi}) - e^{-|z-vt|/\xi}] \\ &= \eta_{ss}(z) + \eta ds(z, t),\end{aligned}\quad (2)$$

where z is the distance into the film from the photoexcited film surface, v is the longitudinal sound velocity, K is a constant proportional to the heat transferred to the film from the pump pulse, and ξ is the optical penetration depth at $\hbar\omega(\text{pump})$. In Eq. (2) $\eta_{ss}(z)$ is the static strain that takes the profile of the pump absorbed energy in the film ($e^{-z/\xi}$), whereas $\eta ds(z, t)$ is the dynamic strain wave that bounces from the film interfaces. Assuming poor bonding of the polymer film to the substrate, then $\eta ds(z, t)$ changes its sign at each film interface, thus forming an oscillatory $\Delta T(t)$ response component. It is possible to obtain the sound velocity, v , from the round-trip time given by the oscillation period, where $v = 2d/\tau_T$. From our data, we thus obtain in RR-PTV $v \approx 1$ nm/ps, which is in good agreement with sound velocities in other polymer films.¹⁰

The TS response is detected through its modulation of the film transmission, $\Delta T_s(t)$, which is proportional to the strain $\eta(t)$ averaged over the film thickness. Thus, $\Delta T_s(t)$ is composed of two components, namely, a time-independent component related to η_{ss} , which is superimposed by an oscillatory component related to $\eta ds(t)$, in agreement with our findings [Figs. 3(a) and 3(b)]. It was previously deduced¹¹ that the TS spectrum $\Delta T_s(\omega) = d\alpha(\omega)/d\omega \Lambda \eta ds(t)d/\hbar$, where Λ is the deformation potential; and therefore the $\Delta T_s(\omega)$ spectrum follows closely that of $d\alpha(\omega)/d\omega$, consistent with our findings [Fig. 3(c), inset].

In summary, we showed that the ultrafast response of RR-PTV is dominated by the fast decay of the photogenerated $1B_u$ excitons into the “dark” $2A_g$ exciton with lower energy; this limits the PLQE to $\sim 2 \times 10^{-4}$. From the measurements of PL, transient PM and EA spectra, we determined the essential states in this NDGS polymer. The ultrafast energy release associated with the exciton decay gives rise to substantial static and dynamic strains in the film that dramatically influence the film’s transient PM response. We conclude that NDGS polymers with intrinsic weak PL may be used in nonlinear optical applications because of their ultrafast response, as well as in transducers for TS spectroscopic studies due to their ultrafast energy release.

The work at the University of South Florida was supported by New Energy Technologies, Inc., and Florida High Tech Corridor Matching Fund (FHT 09-18); the work at the University of Utah was supported by Department of Energy Grant No. ER46109.

*Permanent address: School of Electronic and Optical Engineering, Nanjing University of Science and Technology, Nanjing 210094, China.

†Author to whom correspondence should be addressed: xjiang@usf.edu

¹Z. G. Soos, S. Elemad, D. S. Galvao, and S. Ramasesha, *Chem. Phys. Lett.* **194**, 341 (1992).

²J. H. Burroughes, D. D. C. Bradley, A. R. Brown, R. N. Marks, K. Mackay, R. H. Friend, P. L. Burns, and A. B. Holmes, *Nature (London)* **347**, 539 (1990).

³C.-X. Sheng, M. Tong, S. Singh, and Z. V. Vardeny, *Phys. Rev. B* **75**, 085206 (2007).

⁴A. J. Brassett, N. F. Colaneri, D. D. C. Bradley, R. A. Lawrence, R. H. Friend, H. Murata, S. Tokito, T. Tsutsui, and S. Saito, *Phys. Rev. B* **41**, 10586 (1990).

⁵F. Banishoeib, A. Henckens, S. Fourier, G. Vanhooyland, M. Breselge, J. Manca, T. J. Cleij, L. Lutsen, D. Vanderzande, L. H. Nguyen, H. Neugebauer, and N. S. Sariciftci, *Thin Solid Films* **516**, 3978 (2008).

⁶E. Lafalce and X. Jiang, *J. Phys. Chem. B* **115**, 13139 (2011).

- ⁷C. Giroto, D. Cheyys, T. Aernouts, F. Banishoeib, L. Lutsen, T. J. Cleij, D. Vanderzande, J. Genoe, J. Poortmans, and P. Heremans, *Org. Electron.* **9**, 740 (2008).
- ⁸S. N. Dixit, D. Guo, and S. Mazumdar, *Phys. Rev. B* **43**, 6781 (1991).
- ⁹C. Thomsen, H. T. Grahn, H. J. Maris, and J. Tauc, *Phys. Rev. B* **34**, 4129 (1986).
- ¹⁰G. S. Kanner, Z. V. Vardeny, and B. C. Hess, *Phys. Rev. B* **42**, 5403 (1990).
- ¹¹G. S. Kanner, S. Frolov, and Z. V. Vardeny, *Phys. Rev. Lett.* **74**, 1685 (1995).
- ¹²G. Lanzani, G. Cerullo, M. Zavelani-Rossi, S. DeSilvestri, D. Comoretto, G. Musso, and G. Dellepiane, *Phys. Rev. Lett.* **87**, 187402 (2001).
- ¹³C. Zhang, J. Sun, R. Li, S.-S. Sun, E. Lafalce, and X. Jiang, *Macromolecules* **44**, 6389 (2011); C. Zhang, T. Matos, R. Li, S.-S. Sun, J. E. Lewis, J. Zhang, and X. Jiang, *Polym. Chem.* **1**, 663 (2010).
- ¹⁴J. Clark, C. Silva, R. H. Friend, and F. C. Spano, *Phys. Rev. Lett.* **98**, 206406 (2007).
- ¹⁵M. Liess, S. Jeglinski, Z. V. Vardeny, M. Ozaki, K. Yoshino, Y. Ding, and T. Barton, *Phys. Rev. B* **56**, 15712 (1997).
- ¹⁶Z. V. Vardeny and J. Tauc, *Opt. Commun.* **39**, 396 (1991).
- ¹⁷X. M. Jiang, R. Österbacka, O. Korovyanko, C. P. An, B. Horovitz, R. A. J. Janssen, and Z. V. Vardeny, *Adv. Funct. Mater.* **12**, 587 (2002).
- ¹⁸J. C. deMello, H. F. Wittmann, and R. H. Friend, *Adv. Mater* **9**, 230 (1997).
- ¹⁹H. Sirringhaus, P. J. Brown, R. H. Friend, M. M. Nielsen, K. Bechgaard, B. M. W. Langeveld-Voss, A. J. H. Spiering, R. A. J. Janssen, E. W. Meijer, P. Herwig, and D. M. de Leeuw, *Nature* **401**, 685 (1999).
- ²⁰See Supplemental Material at <http://link.aps.org/supplemental/10.1103/PhysRevB.85.235201> for the fitting of PL spectra and the cross-correlation analysis in transient PA spectra.
- ²¹N. T. Harrison, G. R. Hayes, R. T. Phillips, and R. H. Friend, *Phys. Rev. Lett.* **77**, 1881 (1996).
- ²²J. Orenstein and G. L. Baker, *Phys. Rev. Lett.* **49**, 1043 (1982).